ISSN: 2996-0940
Research Article

Science Set Journal of Ophthalmology and Eye Care

The Performance of two Segmentation Convolutional Neural Networks, U-Net and SegNet, for the Segmentation of Cystoid Macular Edema

Carolyn Yu Tung Wong[1, 2, 3*], Tin Lik Wong[3], Timing Liu[1, 2], and Henry Hing Wai Lau[4]

[1]*Institute of Ophthalmology, University College London, London, United Kingdom*
[2]*Moorfields Eye Hospital NHS Foundation Trust, London, United Kingdom*
[3]*Faculty of Medicine, The Chinese University of Hong Kong, Hong Kong, China*
[4]*Department of Ophthalmology and Visual Sciences, The Chinese University of Hong Kong, Hong Kong, China*

[*]Corresponding author: Carolyn Yu Tung Wong, Prince of Wales Hospital, 30-32 Ngan Shing Street, Shatin, New Territories, Hong Kong.

Submitted: 24 May 2024 **Accepted:** 27 May 2024 **Published:** 03 June 2024

https://doi.org/10.63620/MKSSJOEC.2024.1012

Citation: *Wong, C. Y. T., Wong, T. L., Liu, T., & Lau, H. H. W. (2024). The Performance of two Segmentation Convolutional Neural Networks, U-Net and SegNet, for the Segmentation of Cystoid Macular Edema. Sci Set J of Ophthalmology & Eye Care, 3(2), 01-07.*

Abstract

Background: *Screening is the primary method used to detect cystoid macular edema in conditions that threaten vision, such as diabetic retinopathy and age-related macular degeneration. However, the interpretation of imaging data relies heavily on the expertise of ophthalmologists, leading to subjective factors. The integration of computer-aided diagnostics as a secondary tool has helped to decrease diagnostic uncertainties among doctors. Therefore, the refinement of these systems, particularly in terms of more precise segmentation and disease detection, is crucial. In this study, two well-known convolutional neural networks (CNNs), U-Net and SegNet, were utilized for segmenting intraretinal fluid in optical coherence tomography (OCT) images for diagnosing cystoid macular edema (CME). Determining the most suitable architecture for this task can alleviate the burden on ophthalmologists during CME screenings and triage.*

Methods: *CNNs are employed in segmentation to categorize individual pixels in an image based on self-learned weights. In this study, we utilized 80 OCT images of cystoid macular edema (CME) along with their respective masks obtained from the Liaquat University of Medical and Health Sciences dataset. We evaluated the efficacy of automatic segmentation conducted by U-Net and SegNet with various configurations in the task of intraretinal fluid segmentation relevant to CME diagnosis.*

Results: *Out of the two suggested architectures, U-Net demonstrated superior performance, achieving an accuracy of 0.9984, a dice coefficient of 0.8478, and requiring less training time compared to SegNet. In contrast, SegNet achieved an accuracy of 0.9961 and a dice score of 0.5502.*

Conclusion: *Depending on their setup, both networks can accurately segment OCT images of CME, with U-Net typically demonstrating quicker training times and higher accuracy levels.*

Keywords: Artificial Intelligence, Image Segmentation, Cystoid Macular Edema, Optical Coherence Tomography

Introduction

Cystoid macular edema (CME) is a common pathologic sequel of the retina and can manifest in various pathological situations like intraocular inflammation, central or branch retinal vein occlusion, age-related macular degeneration (AMD) and diabetic retinopathy (DR) [1]. DR and AMD have become primary contributors to irreversible blindness in patients with the projected number of individuals to experience vision loss doubling in the next three decades [2]. Optical coherence tomography (OCT) offers excellent visualization of cystoid fluid by utilizing non-invasive, low-coherence light to capture optical reflections from internal structures within biological tissues [3, 4]. The effectiveness of OCT in visualizing CME is highlighted by its ability to distinguish cystoid fluid from surrounding retinal tissues due to lower optical scattering [5-7]. While conventional OCT-based assessments in CME-related disorders typically focus on mea-

suring foveal thickness, recent research indicates that CME can occur without macular thickening in certain retinal conditions [8]. Additionally, measurements of macular thickness may be less accurate in the presence of subretinal fluid [9, 10]. In fact, it is challenging to manually measure the macular thickness due to time and labour constraints.

To address this issue, researchers have explored fully automated segmentation techniques to detect and quantify microstructural changes in retinal OCT images. Various artificial intelligence (AI) algorithms, including deep learning (DL) models, have been developed to process OCT images and other ophthalmic imaging modalities for disease classification, staging, and feature extraction [11-14]. Fully convolutional neural networks (FCNs) like U-net and SegNet have shown promise in segmenting retinal fluid from OCT images, with some models achieving high accuracy in segmenting intra-retinal cystoid fluid and subretinal fluid [15-17]. DL methods have also been used to measure fluid volume for clinical trial assessments and segment nerve fibre layer thickness and ellipsoid zone disruption [18, 19]. These advancements in AI technology hold potential for improving the diagnosis and management of various eye diseases, including DR and AMD.

Image segmentation enables a more precise and straightforward examination of cystoid fluid and retinal abnormalities. It plays a crucial role in computer-assisted screening for CME by allowing for accurate differentiation and classification of lesions from the background. Ongoing research is focused on enhancing the accuracy of CME image segmentation through the utilization of various architectures, functions, and methods. The primary objective is to enhance the analytical capabilities and precision of computer-assisted diagnostic systems for CME diagnosis and classification. This study represents an initial step towards this goal by evaluating two commonly used and reputable segmentation Convolutional Neural Networks (CNNs), U-Net and SegNet, customized for our CME OCT image dataset. The aim is to precisely isolate the areas of cystoid fluid in OCT images. By training both networks with different activation units and loss functions, we aim to determine which CNN performs better on this task, comparing the results against segmentation labels created manually by experienced specialists.

Methods

We endeavored to carry out the study following the Transparent Reporting of a Multivariable Prediction Model for Individual Prognosis or Diagnosis Standards [20]. To accurately present the essential terms and findings, we referred to the recently introduced Consolidated Standards of Reporting Trials-AI extension (designed for reporting clinical trials involving AI) [21].

OCT images and their associated masks for CME segmentation were obtained from the publicly accessible Liaquat University of Medical and Health Sciences (LUMHS) database [22]. These data were used to train two segmentation networks, namely U-Net and SegNet, for the purpose of CME segmentation. Subsequently, the performance of these two trained networks was compared against each other.

Dataset

The LUMHS dataset is a publicly accessible dataset containing OCT images and ground truth labels for CME [22]. All 80 images within the dataset were sourced from databases at LUMHS and the Institute of Ophthalmology, Jamshoro. These images were organized and classified under the guidance of medical professionals at LUMHS who are skilled in identifying CME and its progression, providing authoritative CME diagnoses. Each pixel in the OCT images was assigned a specific clinical class corresponding to a particular disease, essential for semantic segmentation. Manual binary image masking was carried out using the Image Segmentation tool in MATLAB software, which offers various tools (such as flood fill and freehand drawing) for manually selecting regions of interest in the images. This process was crucial for training our models to detect and isolate CME, as well as validating the accuracy of the digitally selected ROIs for CME.

The mask image designates pixels with a value of "1" as the foreground representing CME, while pixels with a value of "0" indicate the background. These serve as the ground truth labels for the input CME image, which the model must accurately predict. Although a team of medical experts annotated the images for CME labeling, the potential for subjective bias exists as no external expert participated in the annotation process. To expedite training, the images were resized to 224 x 224 pixels and saved in JPEG format during preprocessing. Contrast enhancement and speckle reduction were omitted during preprocessing to assess the networks' capacity to independently and authentically learn image features. Additionally, re-annotation was avoided to prevent bias, given the absence of external annotators and blinding.

The 80 images were split into three subsets: training, validation, and test, with allocations of 70%, 10%, and 20%, respectively. Data augmentation was omitted to reduce computational expenses and prevent additional noise in the original dataset. Our focus was solely on evaluating the performance of the U-Net and Seg-Net segmentation networks in segmenting CME, rather than creating a broadly applicable model for deployment. Normalization of the three subsets was conducted using the mean and standard deviation of the training set, assuming that the test set adequately represents the training set and thus shares the same mean and standard deviation.

Hardware and Software

In this study, Python 3.6.8 was utilized as the programming language, along with the TensorFlow and Keras libraries for DL tasks. The testing environment consisted of a LINUX-based PC equipped with an Intel Core i7-7740X CPU running at 4.30GHz, 32 GB of RAM, and a GeForce GTX 1080 Ti graphics card operating at a clock speed of 33 MHz. The Nvidia driver version employed was 390.59. Statistical analysis was conducted using MATLAB R2015a.

U-Net

Developed in 2015 at the University of Freiburg's Computer Science Department, U-Net is a CNN designed to deliver rapid and accurate image segmentation across various biomedical applications. It is structured with a contracting path to capture context and an expanding path for precise localization. The encoder takes the input image and applies two unpadded convolutions, an activation unit, and a max pooling operation with a stride of 2 for downsampling, repeated four times before transitioning

to the decoder. The steps in the expanding path mirror those in the contracting path, involving upsampling of the feature map, concatenation with the corresponding feature map from the contracting path, and two convolutions with activation. U-Net's unique feature is the merging of the map from the contraction path, distinguishing it from other networks. The expanding path aims to combine precise localization with contextual information from the contracting path to generate an accurate segmentation map. The final layer produces an output containing the segmentation result. The U-Net architecture depicted in Figure 1 was utilized in this study for intraretinal fluid segmentation.

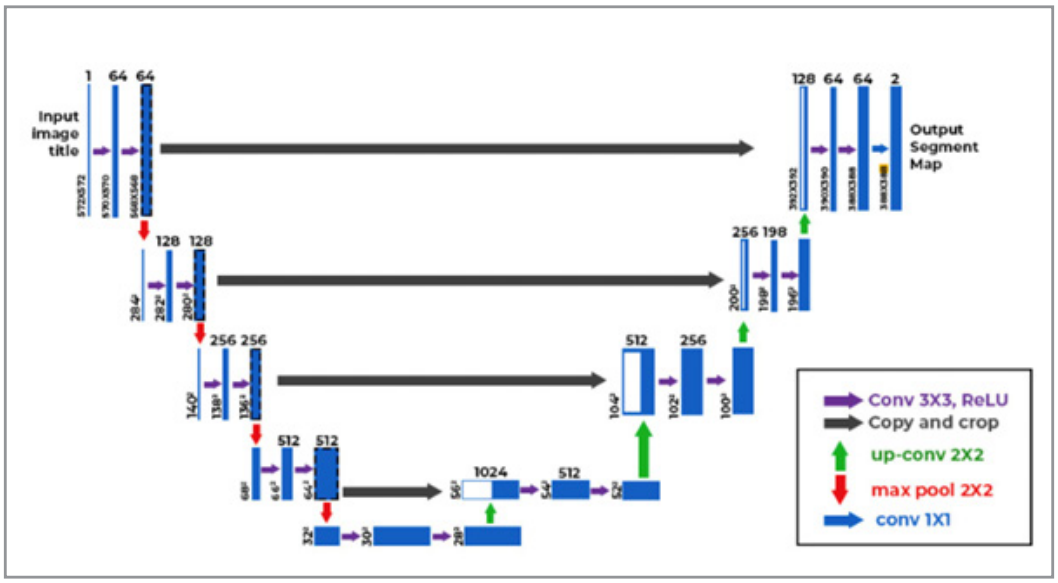

Figure 1: The architecture of the U-Net segmentation network used in this study

SegNet

SegNet is a CNN that shares a similar overall structure with U-Net and was developed by members of the University of Cambridge's Computer Vision and Robotics Group for multi-class pixel-wise segmentation. This network is based on the VGG-16 network layout but has been modified for pixel-wise segmentation tasks. SegNet is known for its ability to achieve high performance scores while utilizing less memory compared to U-Net. The architecture of SegNet differs from U-Net in terms of the number of convolutional layers. In SegNet, the initial two steps involve two convolutions followed by batch normalization and activation before pooling, while the subsequent three steps consist of three convolutions each. The decoder section of SegNet mirrors the encoder but involves upsampling instead of downsampling and a final 1x1 convolution for pixel-wise classification. A key innovation of SegNet is the reuse of pooling indices, where the decoder uses the max pooling indices memorized from the encoder to upsample input feature maps. This approach reduces the memory requirements of the system compared to U-Net, which transfers the entire map. The SegNet architecture depicted in Figure 2 was utilized in this study for segmenting intraretinal fluid.

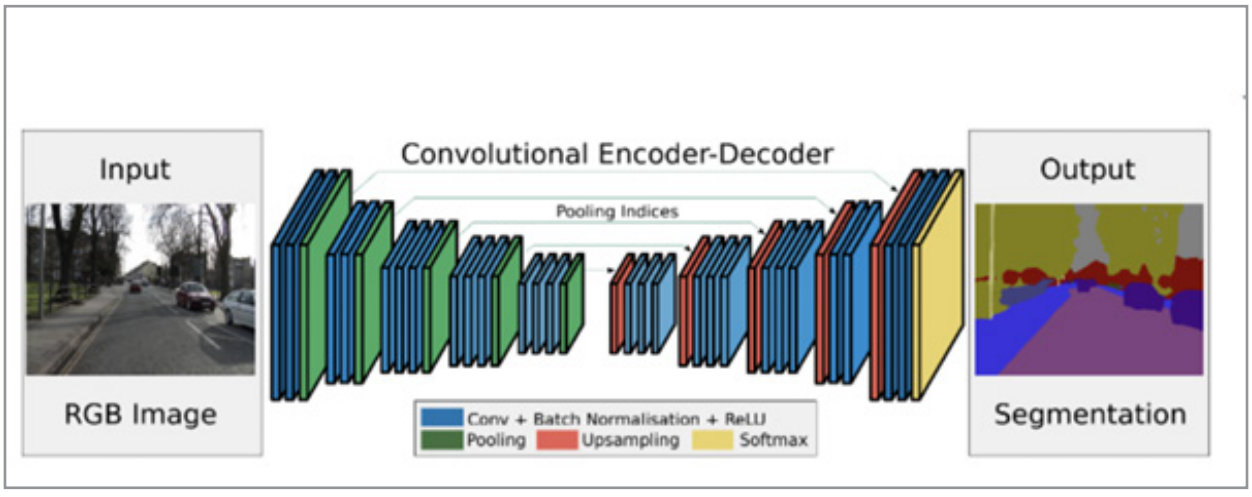

Figure 2: The architecture of the Seg-Net segmentation network used in this study

Network Training, Validation, Testing and Results Extraction
Throughout the process of constructing the segmentation models, we trained the U-Net and Seg-Net networks using the provided 80 OCT images and masks. We made modifications to the kernel size (3 × 3, 5 × 5, and 7 × 7) and learning rate (10-3, 10−5, and 10−6), as well as experimented with activation functions (ReLU and PReLU) and loss functions (dice and cross-entropy). While the original architectures of both networks utilize ReLU and cross-entropy, recent studies have suggested the use of PReLU for improved accuracy and dice loss for addressing pixel imbalance [23, 24]. Additionally, we conducted training for 1,000 epochs in U-Net and 2,000 epochs in SegNet due to the latter requiring more time to stabilize.

We employed 64 pairs of OCT images and masks for training and validation, as per our initial dataset division. The model aims to optimize the training data by reducing the loss function, while the validation set helps fine-tune the parameters. During each training epoch, the model is saved if its validation score surpasses the previous one, and the training data is shuffled to eliminate any presentation order bias. Subsequently, we evaluate each segmentation model using a test set comprising 16 pairs of OCT images and masks.

Every trial is conducted with the goal of creating a model that outperforms its predecessor on the test set. We tested various combinations of batch size, kernel size, dropout rate, and learning rate until identifying the optimal configuration for each network based on its original architecture. Subsequently, we assessed the results obtained from different loss and activation functions.

The segmentation evaluation metrics assess the accuracy of correctly segmented image pixels compared to the ground truth. Various standard evaluation metrics, such as accuracy, precision, recall, and dice score, were computed. True positives (TP) represent correctly identified foreground (white) pixels, while false positives (FP) are incorrectly detected pixels. True negatives (TN) are accurately segmented background (black) pixels, whereas false negatives (FN) are erroneously segmented pixels. Due to the class imbalance issue in CME segmentation, where there are fewer foreground pixels compared to background pixels, achieving high accuracy, such as 90%, may still struggle to accurately classify the class. Therefore, the dice coefficient (F1-score) is commonly used for color image segmentation, measuring the similarity between manually segmented ground truth images and automatically segmented images. The dice coefficient, also referred to as the overlap index, is calculated using the formula 2xTP/(2xTP+FP+FN) and ranges from 0 to 1, with 0 indicating no overlap and 1 indicating complete overlap between predicted and ground truth images.

Results

In evaluating the performance of U-Net and Seg-Net on the LUMHS image subsets, optimal configurations for U-Net included a learning rate of 10–5, a 3 × 3 kernel size, a batch size of 8, and a 50% dropout rate. The average dice scores for testing output images and training times for each activation-loss pair in the U-Net architecture are detailed in Table 1. Conversely, Seg-Net demonstrated superior performance with a 5 × 5 kernel size, a learning rate of 10−6, a 50% dropout rate, and a batch size of 32. Table 2 presents the average dice score in the training set and training duration for the Seg-Net architecture. Figure 3 visually compares manually delineated segmentation masks with the predicted segmentation masks generated by U-Net and Seg-Net using their most effective configurations for intraretinal fluid segmentation.

Table 1: presents the experimental outcomes of U-Net. Each row represents an experiment utilizing a distinct combination of activation and loss functions. The fourth and fifth columns display the average dice score with standard deviation in the test set and the training time of the model in hours, respectively.

Experiment	Activation Unit	Loss function	Average dice score	Training time (h)
1	PReLU	Cross-entropy	0.742±0.130	5.97
2	PReLU	Dice	0.743±0.132	5.97
3	ReLU	Cross-entropy	0.749±0.131	3.95
4	ReLU	Dice	0.751±0.136	3.95

Table 2: displays the experimental findings of Seg-Net. Each row corresponds to an experiment employing a unique combination of activation and loss functions. The fourth and fifth columns indicate the average dice score with standard deviation in the test set and the duration required to train the model in hours, respectively.

Experiment	Activation Unit	Loss function	Average dice score	Training time (h)
5	PReLU	Cross-entropy	0.680±0.146	8.78
6	PReLU	Dice	0.693±0.144	8.78
7	ReLU	Cross-entropy	0.680±0.147	6.96
8	ReLU	Dice	0.693±0.149	6.96

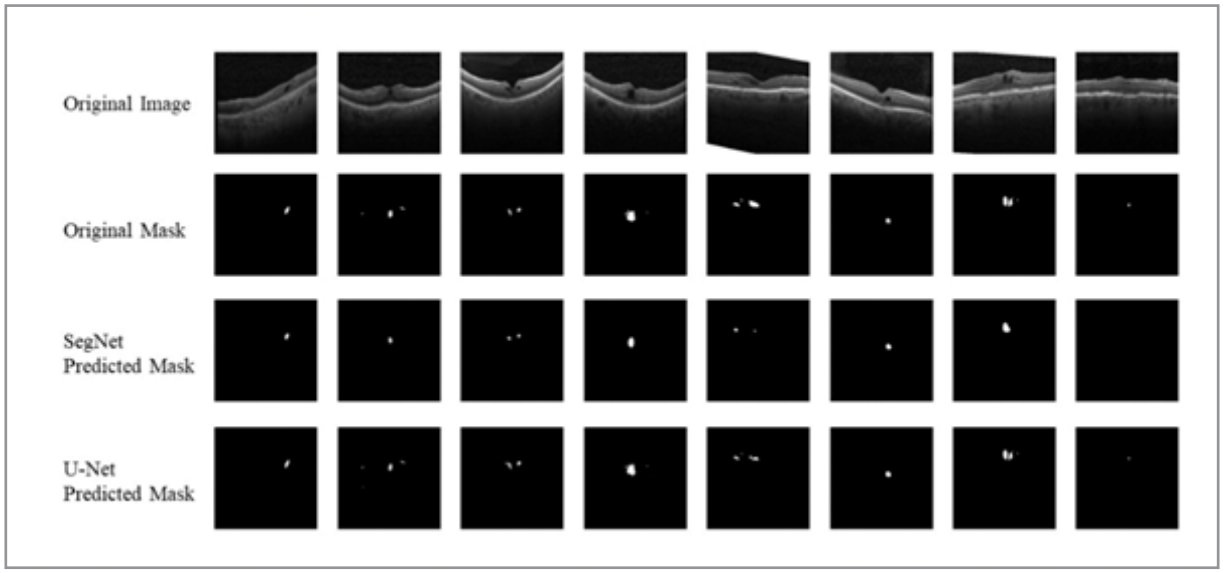

Figure 3: illustrates the comparison among the manually annotated segmentation mask, the segmentation mask generated by U-Net in its optimal configuration, and the segmentation mask produced by Seg-Net in its optimal configuration for cystoid macular edema segmentation. The first two rows display the original image and its corresponding manual label from the test set. The third row exhibits the segmentation output of Seg-Net's most effective configuration, while the fourth row showcases the segmentation output of U-Net's top-performing configuration.

Intraretinal Cystoid Fluid Segmentation

Table 3 displays the performance measurements of U-Net and Seg-Net segmentation models on the LUMHS dataset, utilizing the most effective configurations. U-Net achieved an accuracy of 0.9984, precision of 0.8401, recall of 0.8893, and a dice score of 0.8478. On the other hand, SegNet's segmentation resulted in an accuracy of 0.9962, precision of 0.7505, recall of 0.4989, and dice score of 0.5502.

Table 3: U-Net and Seg-Net performance on intraretinal fluid segmentation in cystoid macular edema

	Accuracy	Precision	Recall	Dice score
U-Net	0.9984	0.8401	0.8893	0.8478
Seg-Net	0.9961	0.7505	0.4989	0.5502

Discussion

The examination of intraretinal fluid in CME is important for identifying and treating various ocular conditions such as AMD and diabetic macular edema [25]. Therefore, the segmentation of intraretinal fluid and the measurement of cystic spaces are crucial for detecting retinal pathology and assessing its severity [25]. In our research, where we compared the effectiveness of a deep U-Net and a Seg-Net segmentation network, we observed that both models could accurately segment intraretinal fluid for diagnosing CME. However, our deep U-Net exhibited superior performance in the task of CME segmentation.

The use of PReLU as an activation function was found to notably prolong the training process for both networks without offering a substantial benefit in terms of improving segmentation accuracy. This effect was particularly noticeable in the performance of the U-Net model, which saw a training time increase of approximately 51.2%. While the intention behind transferring feature maps from the encoder to the decoder in U-Net was to slow down training, adjusting the learning rate and employing heavier filters in SegNet models led to even longer training durations. It is worth noting that the choice of different loss functions did not impact training times. In terms of test time, all models successfully segmented test images in under a second.

In the comparison of label accuracy, U-Net demonstrated superior performance over SegNet in almost all configurations, with the smallest variance being 7.07% in dice scoring. The majority of subpar segmentation results, characterised by lower dice coefficient values, were observed in images with minimal contrast between the lesion and the background, as well as in images containing multiple dark areas. SegNet has a tendency to miss sharp edges, leading to rounded segmentation maps. By examining the dice scores in Table 1 for each model individually, we can observe that the largest difference among different versions of U-Net is as minimal as 1.21%, whereas the difference in SegNet is 1.91%, as depicted in Table 2.

From a clinical perspective, our results could lay the groundwork for future investigations into the creation of AI-assisted systems for screening CME and classifying diseases that pose a threat to vision, such as DR and AMD. In these conditions, the

accurate segmentation of intraretinal fluid is crucial for characterising features in these systems to aid in diagnosis, monitoring, and the development of personalised management strategies and follow-up plans [26-28]. These AI systems have the potential to overcome current challenges in CME diagnosis and treatment, including a lack of specialists and subjective differences in the clinical recognition of essential DR diagnostics [26-28].

Limitations

However, our system faced a potential limitation due to the input images. With only 80 CME images available, the segmentation models may have been constrained in achieving their maximum performance potential. We exclusively utilized high-quality OCT images from the LUMHS dataset, but variations in images could arise from differences in devices. Additionally, the selected photographs, while of acceptable quality, may not accurately represent reality, potentially leading to the loss of features in lower-quality images. Lastly, concerns exist regarding the quality of the provided ground truths (i.e., segmentation masks created by CME experts) due to the lack of information on annotators' qualifications and the consensus process for addressing inter-observer variability in annotation. The ground truths utilized may have been of suboptimal quality and questionable reliability.

Future Work

In upcoming studies on CME, it is essential to advocate for increased collaboration among regions and hospitals to collect a more diverse range of CME images using different types of equipment. Rather than relying solely on images from a single geographic area, datasets should be expanded to encompass images from various regions, populations, and ethnicities to capture a wider array of features for CME diagnosis. Additionally, we will explore more rigorous, quantitative criteria for image screening and create preprocessing modules to automate and standardise image screening. Furthermore, it would be intriguing to analyse and visualise the features learned by segmentation networks in future research endeavours.

Conclusion

We have successfully developed two convolutional neural networks for segmenting intraretinal fluid in CME OCT images, achieving high accuracies. Through our recommended architectures, we have determined that the U-Net outperforms the SegNet in segmenting our CME OCT datasets. The SegNet requires longer training time and demonstrates a lower dice score, posing a risk of smoothing edges and potentially compromising subsequent diagnoses. While U-Net is a widely used model for medical image segmentation, it did not yield the best results in segmenting intraretinal fluid in our OCT CME images, primarily due to the characteristics of our CME OCT image collections. To enhance segmentation accuracy, adjustments to the size and diversity of the OCT datasets would be necessary.

Our present research focuses on evaluating the performance of two established segmentation networks based on their setups for the crucial task of segmenting CME in diagnostics and disease classification. The objective is to offer a benchmark for future researchers looking to create segmentation-based systems for CME diagnosis and screening. In the upcoming period, it will be beneficial to compare various segmentation methods and networks, including GAN and attention-gated U-Net, using the identical CME OCT dataset to identify the most effective segmentation network for precise CME segmentation.

Conflict of Interest

All authors have disclosed no conflict of interests

Funding/ Support

This study received no specific grant from any funding agency in the public, commercial, or not-for-profit sectors.

Data Availability Statement

All data is publicly available and can be retrieved from open-source platforms like Google Dataset Search and Kaggle. The link to the dataset used was also cited in the reference.

Ethics Statements and Patient Consent for Publication

Not required

Reference

1. Rotsos, T. G., & Moschos, M. M. (2008). Cystoid mac ular edema. Clin Ophthalmol, 2, 919-930.
2. Wilkins, G. R., Houghton, O. M., & Oldenburg, A. L. (2012). Automated segmentation of intraretinal cystoid fluid in optical coherence tomography. IEEE Trans Biomed Eng, 59, 1109-1114.
3. Huang, D., Swanson, E. A., Lin, C. P., Schuman, J. S., Stinson, W. G., et al. (1995). Imaging of macular diseases with optical co herence tomography. Ophthalmology, 102, 217-229.
4. Puliafito, C. A., Hee, M. R., Lin, C. P., Reichel, E., Schuman, J. S., et al. (1995). Imaging of macular diseases with optical coher ence tomography. Ophthalmology, 102, 217-229.
5. Hee, M. R., Puliafito, C. A., Duker, J. S., Reichel, E., Coker, J. G., et al. (1998). Topography of diabetic macular edema with optical coherence tomography. Ophthalmology, 105, 360-370.
6. Otani, T., Kishi, S., & Maruyama, Y. (1999). Patterns of diabetic macular edema with optical coherence tomography. Am J Ophthalmol, 127, 688-693.
7. Alex David, S., Mahesh, C., Dhilip Kumar, V., Kemal Polat, Adi Alhudhaif, et al. (2022). Retinal Blood Vessels and Op tic Disc Segmentation Using U-Net. Math Probl Eng, 2022, 8030954.
8. Jun, J. J., Duker, J. S., Baumal, C. R., McCabe, F., Reichel, E., et al. (2010). Cystoid macular edema without macular thickening: a retrospective optical coherence tomographic study. Retina, 30, 917-923.
9. Sadda, S. R., Wu, Z., Walsh, A. C., Richine, L., Dougall, J., et al. (2006). Errors in retinal thickness measurements obtained by optical coherence tomography. Ophthalmology, 113, 285-293.
10. Keane, P. A., Mand, P. S., Liakopoulos, S., Walsh, A. C., & Sadda, S. R. (2009). Accuracy of retinal thickness measurements ob tained with Cirrus optical coherence tomography. Br J Oph thalmol, 93, 1461-1467.
11. Hwang, D. K., Hsu, C. C., Chang, K. J., Chao, D., Sun, C. H., et al. (2019). Artificial intelligence-based decision-making for age-related macular degeneration. Theranostics, 9, 232-245.

12. Kermany, D. S., Goldbaum, M., Cai, W., Valentim, C. C. S., Liang, H., et al. (2018). Identifying Medical Diagnoses and Treat able Diseases by Image-Based Deep Learning. Cell, 172, 1122-1131.
13. Yoo, T. K., Choi, J. Y., & Kim, H. K. (2021). Feasibility study to im prove deep learning in OCT diagnosis of rare retinal diseas es with few-shot classification. Med Biol Eng Comput, 59, 401-415.
14. Arsalan, M., Haider, A., Won Lee, Y., & Ryoung Park, K. (2022). Detecting retinal vasculature as a key biomarker for deep Learning-based intelligent screening and analysis of dia betic and hypertensive retinopathy. Expert Syst Appl, 200, 117009.
15. Kugelman, J., Alonso-Caneiro, D., Read, S. A., Vincent, S. J., & Collins, M. J. (2018). Automatic segmentation of OCT reti nal boundaries using recurrent neural networks and graph search. Biomed Opt Express, 9, 5759-5777.
16. Pekala, M., Joshi, N., Liu, T. Y. A., Bressler, N. M., DeBuc, D. C., et al. (2019). Deep learning based retinal OCT segmentation. Comput Biol Med, 114, 103445.
17. Roy, A. G., Conjeti, S., Karri, S. P. K., Sheet, D., Katouzian, A., et al. (2017). ReLayNet: retinal layer and fluid segmentation of macular optical coherence tomography using fully convolu tional networks. Biomed Opt Express, 8, 3627-3642.
18. Schmidt-Erfurth, U., Mulyukov, Z., Gerendas, B. S., Reiter, G. S., Lorand, D., et al. (2023). Therapeutic response in the HAWK and HARRIER trials using deep learning in retinal fluid vol ume and compartment analysis. Eye, 37, 1160-1169.
19. Roberts, P. K., Vogl, W. D., Gerendas, B. S., Glassman, A. R., Bo gunovic, H., et al. (2020). Quantification of Fluid Resolution and Visual Acuity Gain in Patients with Diabetic Macular Edema Using Deep Learning: A Post Hoc Analysis of a Randomized Clinical Trial. JAMA Ophthalmol, 138, 945 953.
20. Collins, G. S., Reitsma, J. B., Altman, D. G., & Moons, K. G. M. (2015). Transparent reporting of a multivariable prediction model for individual prognosis or diagnosis (TRIPOD): the TRI POD statement. BMJ, 350, h5861.
21. Liu, X., Cruz Rivera, S., Moher, D., Calvert, M. J., & Denniston, A. K. (2020). SPIRIT-AI and CONSORT-AI Working Group. Re porting guidelines for clinical trial reports for interventions involving artificial intelligence: the CONSORT-AI exten sion. Nat Med, 26, 1364-1374.
22. Ahmed, Z. (2022). Intraretinal Cystoid Fluid. https://www.kaggle.com/datasets/zeeshanahmed13/intraretinal-cystoid-fluid
23. He, K., Zhang, X., Ren, S., & Sun, J. (2015). Delving Deep into Rectifiers: Surpassing Human-Level Performance on Ima geNet Classification. arXiv.
24. Sudre, C. H., Li, W., Vercauteren, T., Ourselin, S., & Jorge Cardo so, M. (2017). Generalised Dice Overlap as a Deep Learning Loss Function for Highly Unbalanced Segmentations. Deep Learn Med Image Anal Multimodal Learn Clin Decis Sup port, 240-248.
25. Girish, G. N., Anima, V. A., Kothari, A. R., Sudeep, P. V., Roychow dhury, S., et al. (2018). A benchmark study of automated in tra-retinal cyst segmentation algorithms using optical co herence tomography B-scans. Comput Methods Programs Biomed, 153, 105-114.
26. Mehta, N., Lee, C. S., Mendonça, L. S. M., Raza, K., Braun, P. X., et al. (2020). Model-to-Data Approach for Deep Learning in Optical Coherence Tomography Intraretinal Fluid Segmen tation. JAMA Ophthalmol, 138, 1017-1024.
27. de Moura, J., Samagaio, G., Novo, J., Almuina, P., Fernández, M. I., et al. (2020). Joint Diabetic Macular Edema Segmenta tion and Characterization in OCT Images. J Digit Imaging, 33, 1335-1351.
28. Wu, J., Niu, S., Chen, Q., Fan, W., Yuan, S., et al. (2020). Auto mated segmentation of intraretinal cystoid macular edema based on Gaussian mixture model. J Innov Opt Health Sci, 13, 1950020.